Articles

Human Topoisomerase I Inhibition: Docking Camptothecin and Derivatives into a Structure-Based Active Site Model†

Gary S. Laco,‡ Jack R. Collins,§ Brian T. Luke,§ Heiko Kroth,|| Jane M. Sayer,|| Donald M. Jerina,|| and Yves Pommier*,‡

Laboratory of Molecular Pharmacology, Division of Basic Sciences, National Cancer Institute, Laboratory of Bioorganic Chemistry, National Institute of Diabetes and Digestive and Kidney Diseases, National Institutes of Health, Bethesda, Maryland 20892, and Advanced Biomedical Computing Center, National Cancer Institute−Frederick/SAIC, Frederick, Maryland 21702

Received September 10, 2001; Revised Manuscript Received November 9, 2001

ABSTRACT: Human topoisomerase I (top1) is an important target for anti-cancer drugs, which include camptothecin (CPT) and its derivatives. To elucidate top1 inhibition in vitro, we made a series of duplex DNA substrates containing a deoxyadenosine stereospecifically modified by a covalent adduct of benzo[*a*]pyrene (BaP) diol epoxide [Pommier, Y., et al. (2000) *Proc. Natl. Acad. Sci. U.S.A. 97,* 10739−10744]. The known orientation of the hydrocarbon adduct in the DNA duplex relative to the top1 cleavage site, in combination with a top1/DNA crystal structure [Redinbo, M. R., et al. (1998) *Science 279,* 1504−1513], was used to construct a structure-based model to explain the in vitro top1 inhibition results obtained with adducted DNA duplexes. Here we experimentally determined that the lactone form of CPT was stabilized by an irreversible top1/DNA covalent complex. We removed the BaP moiety from the DNA in the published model, and docked the lactone forms of CPT and derivatives into the top1/DNA active site cavity. The docked ligands were minimized, and interaction energy scores between the ligands and the top1/DNA complex were determined. CPT docks perpendicular to the DNA backbone, projects outward from the major groove, and makes a network of potential H-bonds with the active site DNA and top1 residues, including Arg364, Lys532, and Asn722. The results are consistent with the known structure−activity relationships of CPT and derivatives. In addition, the model proposed a novel top1/N352A "resistance" mutation for 10-OH derivatives of CPT. The in vitro biochemical characterization of the top1/N352A mutant supported the model.

Human topoisomerase I (top1)[1] is a prime target for anti-cancer drugs, because of its pivotal role in relaxing supercoiled DNA for replication and transcription (*1*−*3*). Camptothecin (CPT) is an important top1 inhibitor, and was isolated in the 1960s from the Chinese tree *Camptotheca acuminata* (*4*). Water-soluble CPT derivatives (topotecan and CPT 11) have been introduced in the clinic for colon and ovarian carcinoma (*5*, *6*). CPT 11 is a prodrug of SN-38 (Table 1).

Top1 relaxes DNA by attacking a backbone phosphate with the active site tyrosine (Tyr723, human top1), resulting in a 3′-phosphate−tyrosine bond to the 3′ end of the −1 cleavage site nucleoside, and a free 5′OH on the +1 cleavage site nucleoside (*7*−*9*). Top1 subsequently religates the cleaved DNA, and it is this step that CPT inhibits (*3*, *10*). In the cell, CPT-stabilized top1/DNA cleavage complexes generate cytotoxic double-strand DNA breaks after collision with replication forks (*11*−*16*). CPT-resistant cells have been selected in cell culture, with seven CPT-resistant top1 mutations identified close to the top1/DNA active site (reviewed in *17*).

To experimentally analyze top1 inhibition in vitro, a series of duplex DNA substrates were prepared containing either a single deoxyadenosine (dA) or a deoxyguanosine (dG) residue modified at N^6 or N^2, respectively, by stereospecific formation of a covalent adduct with the polycyclic aromatic hydrocarbon metabolite benzo[*a*]pyrene 7,8-diol 9,10-epoxide (BaP DE). BaP DE adducts at or near the normal top1 cleavage site allowed top1 cleavage, but inhibited subsequent religation (*18*, *19*). The orientations of the BaP moiety of these adducts, in duplex DNA, were derived from NMR studies (*20*, *21*). A structure-based model was constructed

† G.S.L. is supported by a National Cancer Institute postdoctoral fellowship, and J.R.C. and B.T.L. have been funded in whole or in part with Federal funds from the National Cancer Institute, National Institutes of Health, under Contract NO1-CO-56000.

* To whom correspondence should be addressed. Phone: 301-496-5944. FAX: 301-402-0752. E-mail: pommier@nih.gov.

‡ Laboratory of Molecular Pharmacology.

§ Advanced Biomedical Computing Center.

|| Laboratory of Bioorganic Chemistry.

[1] Abbreviations: top1, human topoisomerase I; CPT, camptothecin; 7-ClMe-MDO-CPT, 7-chloromethyl-10,11-methylenedioxy-CPT; BaP, benzo[*a*]pyrene; SN-38, 7-ethyl-10-hydroxy-20-*S*-CPT; MDO-CPT, 10,-11-(methylenedioxy)-CPT; BaP DE, benzo[*a*]pyrene 7,8-diol 9,10-epoxide in which the benzylic 7-hydroxyl group and epoxide are trans; *trans-R* adduct, trans-opened 10*R*-N^6-dA adduct of benzo[*a*]pyrene 7,8-diol 9,10-epoxide; dA, deoxyadenosine; dG, deoxyguanosine.

10.1021/bi011774a
Published on Web 01/11/2002

(*18*) to rationalize the in vitro inhibition results obtained with these adducted DNAs (*18*).

Three previous models predicted that CPT binds in or near the top1 active site. Fan et al. proposed that CPT intercalates between the cleavage site −1/+1 bases, parallel to the plane of the bases, using a docking program and a hypothetical top1/DNA cleavage complex (*22*), before the top1/DNA crystal structure was available. The second model by Redinbo et al. (*9*) used an X-ray crystal structure of a top1/DNA covalent complex. They manually rotated the +1 base out of the DNA helix and then flipped it 180°; next CPT was manually positioned to stack with the +1 base (*9*). With other DNA-modifying enzymes, the modified base has been observed to be rotated out of the helix, but not flipped over (*23*−*25*). A third model was published recently by Kerrigan and Pilch (*26*) in which CPT intercalates between the +1/−1 base pairs, perpendicular to the plane of the base pairs. The top1 amino acids shown in the model (Arg364, Asp533, Asn722) all result in CPT resistance when mutated (*27*−*30*). However, only Arg364 made potential H-bonds directly to CPT. Moreover, this model does not address the inactivity of CPT carboxylate.

Recently, Stewart et al. (*31*) presented preliminary data on a crystal structure of topotecan in complex with top1 and bound DNA. Topotecan intercalates between the +1/−1 base pairs, parallel to the plane of the base pairs. Topotecan appears to belong to a distinct class of CPT derivatives in that it intercalates in DNA in the absence of top1 and carries a positively charged nitrogen (*32*, *33*).

It has been speculated that CPT could form a covalent complex with the top1/DNA active site by opening of the E-ring (Table 1; *34*, *35*). CPT E-ring opening was examined here in the presence of an irreversible top1/DNA covalent complex, and it was found that the lactone form of CPT was stabilized by the top1/DNA complex (Figure 1). We then determined how the lactone forms of CPT and derivatives dock in the top1/DNA active site with a docking program (Collins, J. R., and Luke, B. T., unpublished data), and a structure-based top1/DNA active site model (see Experimental Procedures, *18*). In this previous model, we had rotated the +1 base out of the DNA helix to explain the experimental results from adducted DNA substrates (*18*). This resulted in the +1 base being trapped in a network of H-bonds with top1 active site residues (*18*). The docking results for CPT and derivatives were then compared to the known structure−activity relationships for the respective compounds to see if a correlation existed between the docking orientation, interaction energy score, and in vitro inhibition of top1. The model was then tested experimentally with top1/N352A, a novel top1 "resistance" mutant for 10-OH derivatives of CPT.

EXPERIMENTAL PROCEDURES

Top1 Expression and Purification. The wild-type (wt) top1 construct is similar to that reported elsewhere (*36*). Briefly, the wt top1 gene was cloned into a baculovirus transfer vector and used to make a recombinant baculovirus following the manufacturer's recommendations (BD-PharMingen, San Diego, CA). The wt top1 was then expressed in TN5 insect cells (HighFive, Invitrogen Corp., San Diego, CA) via the recombinant baculovirus, and purified essentially as described (*37*, *38*). The top1/N352A construct was made using standard procedures, and sequenced to verify the introduced mutation.

Oligonucleotides. An oligonucleotide containing an abasic site at the +1 position of the scissile strand (abasic oligonucleotide) was constructed based on a high-affinity *Tetrahymena* rDNA top1 cleavage site (*39*). The scissile strand sequence is 5′AAAAAGACTt/xGAAAAATTTTT3′, with "/" indicating the cleavage site, t indicating the −1 thymine to which top1 makes a covalent bond, and x denoting the +1 abasic site. The scissile strand was prepared using a DNA synthesizer with 0.1 M 5-*O*-(4,4′-dimethoxytrityl)-1,4-anhydro-2-deoxy-D-ribitol-3-[*O*-(2-cyanoethyl)]-*N*,*N*-diisopropylphosphoramidite (*40*, *41*) in the auxiliary base position. The normal synthesizer protocol was modified by programming one additional set of tetrazole and phosphoramidite delivery steps for the abasic phosphoramidite. The resultant 5′-dimethoxytrityl (DMT) oligonucleotide was purified by HPLC on a Hamilton 7 μm PRP-1 column, 10 × 250 mm, eluted with a linear gradient of acetonitrile (10−50%) in 0.1 M $(NH_4)_2CO_3$ over 15 min; $t_r = 11.3$ min. After removal of the DMT protecting group (80% acetic acid in water, 20 min, rt), the oligonucleotide was purified by HPLC on the Hamilton column and eluted with a linear gradient of acetonitrile (5−11%) in 0.1 M $(NH_4)_2CO_3$ over 30 min. The fraction that eluted at ∼15.5 min was rechromatographed on a Phenomenex LUNA C18(2) column, 4.6 × 250 mm, eluted with the same solvent gradient at 40 °C; $t_r = 14.9$ min. The complementary oligonucleotide containing a thymine opposite the abasic site was obtained commercially. The masses of both oligonucleotides were confirmed by mass spectrometry. Oligonucleotides were annealed to form an abasic duplex as described (*9*).

Top1 in Vitro Assays. A single-stranded 22mer oligonucleotide (TH1 oligo) based on a high-affinity *Tetrahymena* rDNA top1 cleavage site (*39*) was 3′-end-labeled with ^{32}P-cordycepin as described (*18*). The TH1 oligo sequence is 5′AAAAAGACTT/GGAAAAATTTTT 3′. The labeled TH1 oligo was annealed to the complementary strand in 1× annealing buffer (10 mM Tris-HCl, pH 7.8, 100 mM NaCl, 1 mM EDTA) by heating the reaction mixture to 95 °C and cooling overnight to room temperature. The end-labeled oligo duplex substrate (approximately 250 fmol/reaction) was incubated with 2.5 ng of top1 either with or without the indicated inhibitor, for 20 min at 25 °C in reaction buffer (10 mM Tris-HCl, pH 7.5, 50 mM KCl, 5 mM $MgCl_2$, 0.1 mM EDTA, and 15 μg/mL protease-free BSA), in a final volume of 25 μL. Reactions were stopped by addition of sodium dodecyl sulfate (SDS, final concentration 0.5%) and run in denaturing polyacrylamide gels as described (*18*). Imaging and quantification were performed using a PhosphorImager and ImageQuant software (Molecular Dynamics, Sunnyvale, CA). Note: (1) all inhibitor stocks and serial dilutions were in 100% DMSO and were vortexed immediately before each serial dilution and addition of inhibitor to each reaction tube; (2) data points used for quantification were in the linear (dose-responsive) range of the assay. Experiments were replicated.

In Vitro Analysis of CPT E-Ring Opening. To quantitate the CPT E-ring opening in vitro, CPT (10 μM) was incubated alone at 24 °C in 20 mM Tris-HCl, pH 7.4, 3 mM DTT, 5 mM EDTA, with abasic duplex (100 μM), with top1 (90 μM), and with top1 in covalent complex with the abasic

duplex (90 and 100 μM, respectively). After 3 h, reactions were stopped by the addition of ice-cold methanol and centrifuged for 3 min at 12000*g*. An aliquot was then immediately analyzed by HPLC, as described (*42*) with modifications, on a Zorbax Eclipse XDB C18 column, 4.6 $\times$ 250 mm, eluted at 1.2 mL/min with a linear gradient of acetonitrile (20−35%) in triethylamine acetate buffer [2% (v/v), adjusted to pH 5.5] over 15 min (Figure 1). The carboxylate and lactone forms of CPT were monitored at 367 nm. The carboxylate form of CPT has approximately the same response at 367 nm as an equimolar injection of the lactone form, as shown by injections of aliquots of the same CPT sample before and after base treatment (data not shown). All experiments were done in replicates.

Docking Ligands into the Active Site of a Top1/DNA Complex. The docking of CPT and derivatives into the top1 active site cavity consisted of three steps: (1) constructing a cavity; (2) building ligand databases that contain one or more ligands, in one or more conformations; and (3) docking each member of a given ligand database into the cavity. To construct the docking cavity for top1, the hydrocarbon portion of the BaP DE dA adduct in the published top1/DNA active site model (*18*) was removed. Next, an initial seed point was chosen within this modified top1/DNA active site model. The docking program then stepped along each coordinate axis and determined if each new point lies within the cavity, has penetrated into the protein, or has extended out into the solvent. Once a set of cavity points was determined, each point was then "pre-loaded" with energy terms obtained from the ECEPP/2 empirical potential (*43*, *44*). The resulting "grid points" were generated to significantly reduce the time needed to calculate the interactions of a particular ligand orientation during the docking simulation.

Next, the geometry of each ligand was completely optimized using Mopac7 under AIX (*45*). Since this version of Mopac7 has the ability to search the potential energy surface, in certain cases multiple optimized structures are obtained. The coordinates and Mulliken partial charges of each unique structure were then stored in a database. The search program (unpublished data) then docked each ligand, from a given database, onto the set of grid points that represent the top1 cavity. For each orientation of the ligand in the cavity, a score was determined. This score is related to an intermolecular interaction energy (between the ligand and enzyme), but also contains additional terms. The nonbonded, hydrogen-bonded, and electrostatic components of the score were obtained from the ECEPP/2 empirical energy function (*43*, *44*). Terms were also included which try to place as much of the ligand as possible within the cavity, and which do not allow any of the ligand to penetrate into the enzyme. In contrast, the ligand was allowed to extend into the solvent without any affect on the score.

During the early stages of the docking run, an Evolutionary Programming method (*46*) was used to orient the inhibitor within the cavity. At the beginning, the penalty for penetrating into the enzyme was set to zero, and was increased linearly as the docking simulation proceeded. After the Evolutionary Programming procedure found good initial orientations, a local optimizer (*47*) was used to orient the substrate within the cavity.

Table 1: CPT and Derivatives Relative Top1 Inhibition

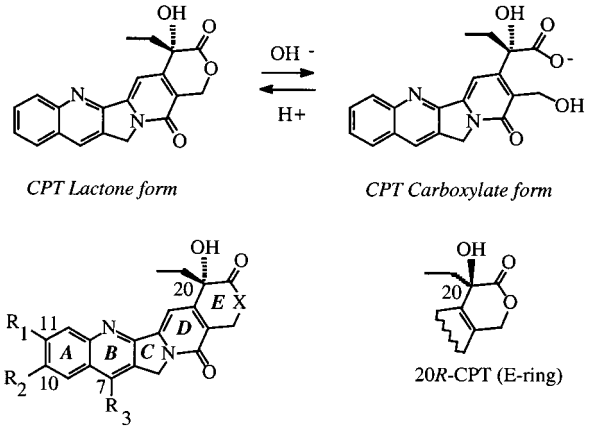

	R_1	R_2	R_3	X	top1 inhibition
CPT	H	H	H	O	+
SN-38	H	OH	$-CH_2-CH_3$	O	++
10-OH-CPT	H	OH	H	O	++
MDO-CPT	$-O-CH_2-O-$		H	O	+++
21-lactam-20*S*-CPT	H	H	H	N	−
20*R*-CPT	H	H	H	O	−

Active Site/Ligand Minimization and Energy Calculations. The AMBER all-atom energy force field (*48*, *49*) was used in all molecular mechanics calculations, and all minimizations were performed using the SANDER-classic module of AMBER6 (*50*). The energy minimization used a 9 Å cutoff and a dielectric constant of 1, and was terminated when the derivative root-mean-square (DRMS) value fell below 0.5. The initial model of top1/DNA was used as the starting model for the energy calculations. The top1/DNA system was energy-minimized without the inhibitors in an effort to relax the structure prior to the full complex calculations. The top1 inhibitors were individually optimized at the nonlocal density functional (Becke−Perdew) double-ζ, valence polarization basis level of theory, as implemented in the dgauss program in UniChem version 5.0 (*51*). Charges for CPT, 20*R*-CPT, SN-38, and 21-lactam-20*S*-CPT were derived from electrostatic potential fits of the density functional wave functions (*51*). Prep input files for CPT and analogues were built using the LEaP program in AMBER. Energy parameters for bond angles not found in the standard force field were approximated by taking closely related parameters found in the parm99 force field (*49*). Energy minimization of the complexes was performed starting from the docked positions of CPT, SN-38, and 20*R*-CPT. The starting structure for the lactam analogue of CPT was obtained by superimposing it onto CPT in the CPT/top1/DNA-minimized complex.

RESULTS AND DISCUSSION

CPT E-Ring Conformation. To define the form of CPT and derivatives that are most likely present in the top1/DNA active site (i.e., lactone versus carboxylate, Table 1), the interaction of the top1/DNA complex with CPT was tested experimentally. Whereas exogenously supplied CPT carboxylate is inactive (*52*−*54*), this does not rule out the possibility that when the CPT lactone enters the top1/DNA active site, E-ring opening is activated (*35*, *55*). We tested CPT E-ring opening in the presence of buffer alone (pH 7.4),

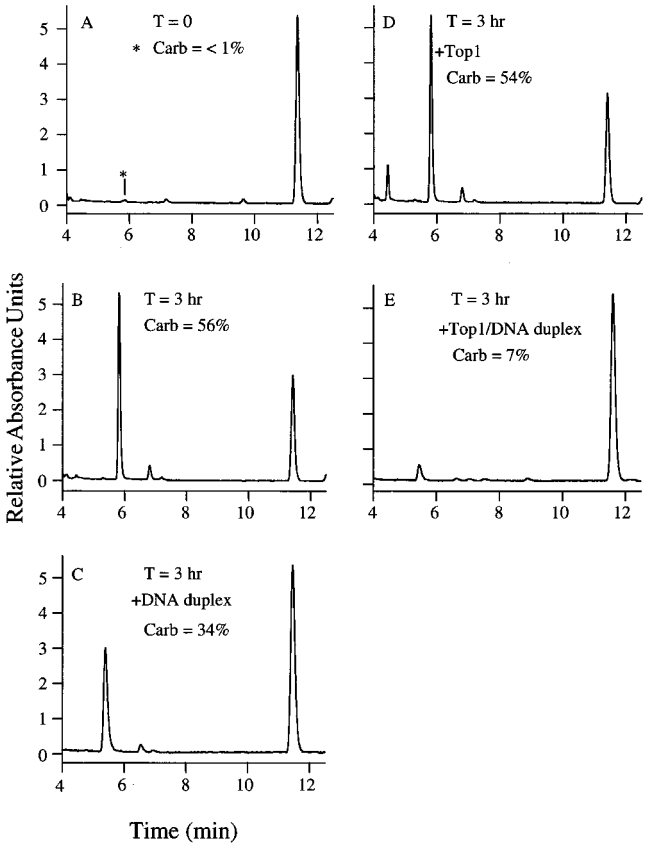

FIGURE 1: Analysis of CPT E-ring opening via HPLC, with detection at 367 nm. The CPT carboxylate (Carb) and lactone forms eluted at 5.4 and 11.4 min, respectively. Except for panel A ($T = 0$), all samples were incubated in buffer at 24 °C for 3 h (see Experimental Procedures). (A) CPT $T = 0$ control; (B) CPT buffer control; (C) CPT and DNA duplex; (D) CPT and top1; (E) CPT and top1/DNA duplex. The percentages of CPT carboxylate (Carb) are given.

an abasic oligonucleotide duplex (DNA duplex), top1, and a top1/DNA duplex irreversible cleavage complex (Experimental Procedures). It should be noted that top1 forms an irreversible complex with the DNA duplex (*56*), thus fixing top1's position with respect to the DNA duplex.

In buffer alone at pH 7.4, 56% of the carboxylate form of CPT accumulated (Figure 1B), and this is consistent with previous reports (*32*, *57*). For CPT and six-membered E-ring lactone derivatives, E-ring hydrolysis is pH-dependent, with E-ring hydrolysis occurring above pH 7 and reversing at acidic pHs (*58*). Under the same conditions, the DNA duplex partially stabilized the CPT lactone in the absence of enzyme (Figure 1C). This result is consistent with the acidic nature of DNA, and the reported stabilization of the CPT lactone by DNA (*32*, *59*). While it is known that CPT does not intercalate in native duplex DNA (*10*, *59*, *60*), we cannot rule out the possibility that a fraction of the CPT binds in the abasic site present in the DNA duplex and is thus protected.

Interestingly, the top1/DNA duplex complex markedly stabilized the lactone form of CPT with only 7% hydrolyzing to form CPT carboxylate (8-fold less carboxylate than in the buffer control, Figure 1, compare panels B and E), whereas the reaction mixture containing top1 accumulated as much CPT carboxylate as the buffer control (Figure 1, compare panels B and D). Because the top1/DNA duplex complex efficiently stabilized the CPT E-ring, the lactone forms of CPT and derivatives were used in the docking experiments presented below.

Top1/DNA Active Site Model. In a recent model of top1 inhibition by DNA containing a trans-opened 10*R*-N^6-dA adduct of benzo[*a*]pyrene 7,8-diol 9,10-epoxide (*trans-R* adduct) at position −1 on the nonscissle strand, we proposed that the cleavage site +1 base on the scissile strand rotated out of the helix to be trapped in a network of H-bonds via Asp533, Arg488, and Arg590 (*18*). The rotated +1 base was then predicted to be prevented from reinserting into the helix by the presence of the intercalated *trans-R* adduct. This model was used to explain why some DNAs containing polycyclic aromatic BaP DE dA adducts, which intercalate in the DNA helix, are irreversible inhibitors of top1 religation (*18*). To generate the docking cavity used here, we removed the *trans-R* adduct from the −1 nonscissile strand base. This resulted in a sizable binding site in the top1/DNA active site, since the +1 base had already been rotated out of the helix (Figure 2, *18*). CPT and derivatives were then docked into the top1/DNA active site cavity (Experimental Procedures). In Table 1, CPT and derivatives that were docked are listed as are their relative in vitro effectiveness as inhibitors of top1 religation.

CPT and SN-38 Docking Orientations in the Top1/DNA Active Site. Since CPT and SN-38 dock in the same orientation and differ by the addition of a 7-ethyl and 10-OH on SN-38, we selected only the SN-38 dock for presentation (Figure 2A). SN-38 docks in the top1/DNA active site cavity perpendicular to the main axis of the DNA, parallel to the bases, and projects outward from the major groove (Figure 2A). The SN-38 D-ring stacks on top of the −1 base (scissile strand) within π-bonding distance, the ethyl group on the E-ring sits underneath the +2 base of the scissile strand (in the space vacated by the rotated +1 scissile strand guanine), while the A-ring projects toward Asn352.

The current model is consistent with the strong SN-38 and CPT preference for a +1 scissile strand purine. The rotated +1 guanine base (scissile strand) leaves a cavity under the +2 scissile strand base which the SN-38 E-ring ethyl group fills in this model (Figure 2). A +1 scissile strand pyrimidine would leave a smaller cavity, and the complementary +1 nonscissile strand purine would then clash with the SN-38 20-ethyl group as presented in this model (data not shown).

When the 10 highest scoring docks of CPT were superimposed, CPT was seen to pivot on the E-ring (in the same plane as the E-ring) with the respective A-rings describing an arc, the apex of which approaches Ala351 and Asn352 (data not shown). A prediction was that a CPT derivative with either an H-bond acceptor or a donor on the A-ring would restrain the A-ring via a H-bond to Asn352, and enhance inhibition of top1. SN-38 is such a derivative (Table 1) and is significantly more potent than CPT in vitro (*61*). In our dock, the SN-38 7-ethyl group projects toward Asn430, while the A-ring 10-OH is within H-bonding distance of Asn352 (Figure 2A). The additional H-bond, distal to the D- and E-ring H-bonds, may be responsible for making SN-38 significantly more potent than CPT. When the 10 highest scoring docks of SN-38 were superimposed, it was clear that the A-ring 10-OH does in fact restrict the movement of all SN-38 A-rings to within H-bonding distance of Asn352 (data not shown).

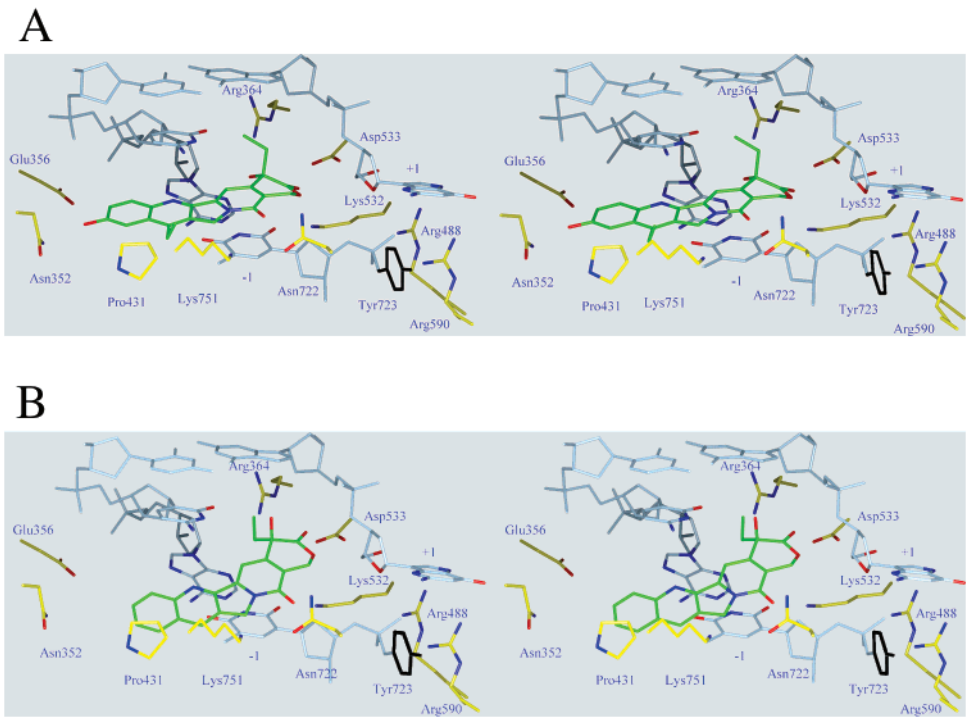

FIGURE 2: Stereoview of minimized ligands in the active site of the top1/DNA covalent complex. The view is looking toward the major groove of the DNA. DNA is light blue, amino acid side chains are yellow, and potential hydrogen bond donating/accepting nitrogens and oxygens are blue and red, respectively. Note that the +1 scissile strand base has been rotated out of the DNA helix. The top1 active site tyrosine (723) is in black and is covalently linked to the −1 scissile strand nucleoside. (A) SN-38 in green, A-ring to the left, E-ring to the right; the 10-OH is on the far left of the A-ring; the 7-ethyl side group is facing the viewer between Pro431 and Lys751; (B) 20*R*-CPT in green, A-ring to the left, E-ring to the right. The 20-ethyl group has been pushed out toward Arg364 by a clash with the −1 nonscissile strand base; the E-ring 20-OH is pointing up toward the +2 scissile strand base.

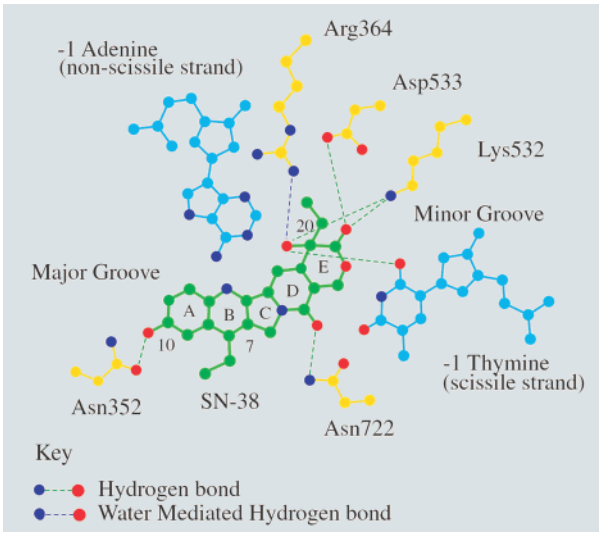

FIGURE 3: Flattened view of Figure 2A, from above. SN-38 in green, and potential H-bonds between SN-38 and top1 amino acids and bound DNA are indicated by dashed lines.

Potential H-Bonds between SN-38 and Top1. The minimized top1/DNA/SN-38 complex was analyzed for H-bonds between top1/DNA and SN-38 using a 3.4 Å cutoff (average H-bond length 3.0 Å), and revealed the following potential H-bonds (Figure 3): (1) The E-ring carbonyl oxygen is within H-bonding distance of Lys532 (an essential residue, *62*) and Asp533. (2) The 20-OH can make a H-bond with Lys532, and the carbonyl oxygen of the −1 scissile strand thymine. While the 20-OH can be replaced with a non-hydrogen-bonding substituent, the 20-OH does have a significant role in CPT binding to top1/DNA complexes, and this is most pronounced at low micromolar drug concentrations (*63*). (3) The D-ring carbonyl oxygen is within H-bonding distance of Asn722. Mutation of Asp722 to Ser results in a CPT-resistant top1 (*30*). (4) The A-ring 10-OH is within H-bonding distance of Asn352 (Figure 3). A potential H-bond outside of the 3.4 Å cutoff includes that between the E-ring 20-OH and Arg364 (4.2 Å); a water molecule could mediate this H-bond. Mutation of Arg364 to His results in a CPT-resistant top1 (*27*).

Interestingly, Asp533 is linked to CPT resistance in top1/D533G (*28*, *29*). In the present model, the CPT resistance of top1/D533G is explained by the fact that the +1 scissile strand nucleoside's free 5′OH cannot be held out of the DNA helix by H-bonding with Gly533 as it is proposed to be with Asp533 (Figure 2; *18*). It has been predicted that when top1/D533G makes a covalent complex with DNA the +1 base can more freely rotate in and out of the helix and so block CPT from binding in the top1/DNA active site (*18*). This prediction is consistent with top1/D533G having a 10-fold higher religation rate than wild-type top1 (*64*). In addition, if the Asp533 carboxylate was protonated, it could make a H-bond with the SN-38 E-ring carbonyl oxygen (3.1 Å), and this would further increase the interaction energy between SN-38 and top1.

Inactive CPT Derivatives. We were interested in understanding why some derivatives of CPT were inactive, and how the docking orientations of those derivatives compared to that of CPT. The 20*R* derivative of CPT is inactive (*52*), and differs from CPT only in the position of the E-ring ethyl and 20-OH groups, which are switched (Table 1). In contrast to CPT and SN-38 for which the 10 highest scoring docks

Table 2: Ligand−Top1/DNA Active Site Interaction Energies

	SN-38	CPT	21-lactam-20*S*-CPT	20*R*-CPT
electrostatic/DNA	−9.52	−6.35	−1.08	8.20
electrostatic/top1	−24.54	−14.47	−11.07	−10.46
vdW/DNA	−40.10	−36.50	−36.96	−32.02
vdW/top1	−11.74	−11.00	−10.82	−11.48
total energies (kcal/mol)[a]	−85.90	−68.32	−59.92	−45.77

[a] The total interaction energies were broken into the electrostatic and van der Waals interactions between each ligand and the DNA and protein (top1) for analysis purposes. vdW, the van der Waals contribution to the interaction energy.

were in similar orientations, when the 10 highest scoring 20*R*-CPT docks were superimposed it was found that there were 2 different orientations (head to tail relative to one another). However, the orientation of the highest scoring 20*R*-CPT dock was somewhat similar to that of SN-38 (Figure 2B). Interestingly, in the case of 20*R*-CPT, the 20-ethyl group is forced out to the side by a clash with the −1 nonscissile strand base. The net effect is to tilt 20*R*-CPT out of the plane of the bases, with a significant loss of π-bonding between the D-ring and −1 base (scissile strand) and H-bond interactions between the 20*R*-CPT E-ring oxygens and the top1/DNA active site (Figure 2B, and data not shown). The poor docking of 20*R*-CPT is reflected in the interaction energy scores (Table 2). The 20*R*-CPT E-ring 20-OH group cannot make the same H-bond/electrostatic interactions in the 20*R* conformation as in the 20*S* (Table 2). In addition, the 20*S*-CPT E-ring 20-ethyl group is predicted to clash with the inward-rotating +1 base, and this may result in CPT being somewhat resistant to displacement by the rotating +1 base (i.e., the clash would drive the 20-ethyl group deeper into the active site). In the case of the 20*R*-CPT, the 20-ethyl group cannot clash with the inward-rotating +1 base (Figure 2B). This proposal is consistent with the loss of activity in CPT derivatives lacking a 20-ethyl group (*65*).

A notable inactive CPT derivative is 21-lactam-20*S*-CPT (Table 1), which is structurally similar to 20*S*-CPT. However, the 21-lactam-20*S*-CPT E-ring cannot open to form a carboxylate due to the E-ring amide nitrogen, a non-H-bond acceptor (*52*). Substitution of the CPT E-ring oxygen with a nitrogen reduces the overall interaction energy for 21-lactam-20*S*-CPT (Table 2), and this indicates that subtle differences can have pronounced effects on inhibitor binding to top1. Thus, the inactivity of the 21-lactam-20*S*-CPT is likely not due to the fact that the E-ring cannot open.

Comparison of the binding energies of SN-38, CPT, 20*R*-CPT, and 21-lactam-20*S*-CPT (Table 2) indicates that SN-38 forms the most stable interactions with the active site, followed by CPT, the 21-lactam-20*S*-CPT, and distantly by the 20*R*-CPT. The breakdown of the interaction energies for each inhibitor correlates with the docking orientation and active site interactions (i.e., SN-38 picks up 10 kcal/mol in electrostatic interactions with top1 because of the extra H-bond between the A-ring 10-OH and Asn352, and the slight movement toward Lys532 which results in a better interaction) (Table 2 and Figure 3).

Additional Structure−Activity Relationships. In the current model, the SN-38 A-ring 10-OH makes a H-bond with Asn352 as would an oxygen in the methylenedioxy moiety of 10,11-(methylenedioxy)-CPT (MDO-CPT), a potent inhibitor of top1 (Table 1, *52*, *53*, *61*). In addition, the model

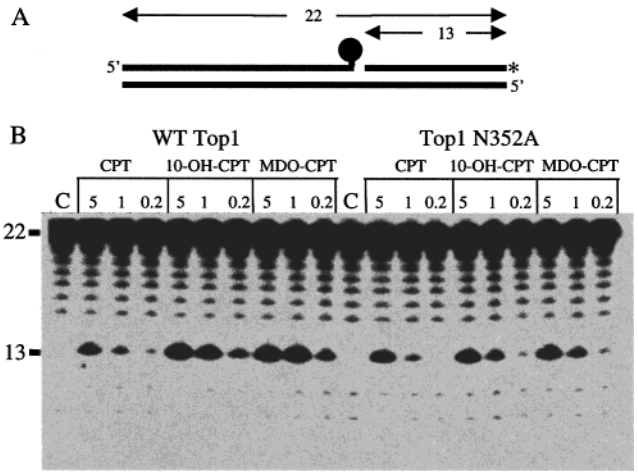

FIGURE 4: Inhibition assay for wt top1 and the N352A mutant. (A) Schematic diagram of top1/DNA cleavage complex; top1 (black sphere) is covalently linked to the 5′ half of the scissile strand, and the end-labeled 13mer reaction intermediate is indicated. (B) Inhibition of top1 religation by CPT and derivatives, and accumulation of the 13mer. Inhibitor concentrations are in micromolar.

accommodates the MDO-CPT methylenedioxy moiety, and explains the low bulk tolerance at position 10 due to the Ala351-Asn352 loop that projects toward the CPT A-ring (Table 1 and Figure 2). Experimentally, substitutions on the CPT A-ring at positions 7 and 9 are well tolerated (*61*), and the model supports these observations. However, even small substitutions at position 12 on the A-ring inactivate CPT derivatives (*52*), consistent with the current model in which the nonscissile strand −1 base restricts the size of a substitution at position 12 on the A-ring.

One CPT derivative, 7-chloromethyl-10,11-methylenedioxy-CPT (7-ClMe-MDO-CPT, *66*), was instrumental in directly defining 7-ClMe-MDO-CPT interaction with the top1/DNA active site. 7-ClMe-MDO-CPT has been shown to alkylate an N-3 nitrogen on a +1 scissile strand purine (*66*). However, this is an inefficient process indicating a suboptimal orientation of the 7-ClMe and the target nitrogen (*66*). In our current model, the +1 guanine nitrogens would come into alkylation "range" of the 7-ClMe when the +1 base re-enters the helix and clashes with the bound 7-ClMe-MDO-CPT.

Experimental Testing of the Model. We tested the role of the top1 Asn352 in making an H-bond with CPT derivatives containing an A-ring 10-OH or equivalent, by making a top1/N352A mutant. Wild-type (wt) top1 and the top1/N352A mutant were assayed on end-labled oligo substrates in the presence of various concentrations of CPT, 10-OH-CPT, and MDO-CPT (Figure 4). The inhibitors block the religation of the top1-cleaved DNA, and result in the reversible accumulation of a 13mer reaction intermediate (Figure 4A,B, *18*). The 13mer reaction intermediate was quantitated for the respective enzyme/inhibitor combinations. Wild-type top1 was inhibited 350% more by 10-OH-CPT and 600% more by MDO-CPT than by CPT (1 μM reactions). We attribute these results to the H-bond that these CPT derivatives are proposed to make with Asn352. Interestingly, the top1/N352A mutant was inhibited only 30% more by both 10-OH-CPT and MDO-CPT than by CPT (5 μM reactions). With this assay, wt top1 is consistently inhibited more by 10-OH-CPT and MDO-CPT than by CPT, while the top1/

N352A mutant is on average inhibited to nearly the same level by all three inhibitors.

CONCLUSIONS

Since the discovery of CPT as an antitumor agent (*4*) and as a specific inhibitor of top1 religation (*10*), attempts have been made to determine the orientation of CPT in the top1/DNA active site (*9*, *22*, *26*). These modeling studies had access to the structure−activity results from numerous derivatives of CPT and top1-resistant mutations (reviewed in *34*). Together these results provided a detailed map of CPT interactions with the top1 active site, and have been used to test models of CPT bound in the top1/DNA active site.

An essential feature of the top1/DNA active site model used for our present docking studies is the rotation of the +1 scissile strand base out of the helix (*18*), as this opens a cavity into which CPT can dock. After top1 makes a covalent complex with supercoiled DNA via the −1 nucleoside (*9*), we propose that as a consequence of top1 releasing the superhelical strain via rotation of the DNA, the +1 nucleoside rotates out of the helix. After each round of "controlled rotation" (*67*), the rotated +1 nucleoside could then H-bond with Arg488, Asp533, and Arg590 (*18*), and so prevent top1 from religating the DNA (Figure 2). This could then result in successive rounds of controlled rotation until enough superhelical strain was released such that the superhelical state of the DNA favored the rotation of the +1 base back into the helix and the "free" 5′OH to within "attacking" distance of the top1/DNA covalent bond. This is consistent with top1 being a processive enzyme (*64*). Once the DNA is completely relaxed, as in a duplex olignucleotide, the +1 base rotation would then be significantly reduced due to the lack of a driving force (i.e., superhelical strain induced DNA rotation). A similar mode of base rotation is used by DNA-modifying enzymes to interact with native duplex DNA (*23*−*25*).

Here we determined experimentally that the lactone form of CPT is preferentially stabilized by the top1/abasic DNA covalent complex (Figure 1). We next presented a model for the top1/DNA active site into which the CPT lactone and derivatives were docked (Figures 2 and 3). The current model of the ternary complex was found to fit the experimentally defined 3-dimensional space accessible around CPT, and was also consistent with the known top1 active site resistance mutations (reviewed in *34*). This approach was based on the hypothesis that CPT and active derivatives bind in similar orientations, with the increased potency of some CPT derivatives being due to better van der Waals interactions and more H-bonds with the top1/DNA active site. It is interesting to note that many of the CPT-resistant top1's have mutations near the top1/DNA active site, and several mutations remove an amino acid that can make an H-bond i.e., Arg364, Asp533, and Asn722 (*27*, *29*, *30*). This suggests that CPT binding is in part dependent on H-bonding interactions with top1. While the models presented here evaluated only CPT and several derivatives, the results defined only one binding orientation for CPT and active derivatives, while inactive CPT derivatives had weaker interactions (Table 2) and consequently less preference in their binding orientations (Results and Discussion). The ligand-top1/DNA active site interaction energies (Table 2) correlate with the experimentally determined in vitro activities of CPT and derivatives (Table 1).

The model also provides new insight into how CPT and derivatives interact with the top1/DNA covalent complex. The docked SN-38 A-ring 10-OH makes a putative H-bond with top1 Asn352 (Figure 3). We demonstrated that mutation of Asn352 to a non-H-bonding Ala residue resulted in a top1/N352A that became sensitive to 10-OH CPT and MDO-CPT to approximately the same level as to CPT (Figure 4, Results and Discussion). The current results indicate that the three previous CPT/top1 models (*9*, *22*, *26*) and the preliminary top1/DNA/topotecan crystal structure (*31*) may not be biochemically relevant for CPT and uncharged derivatives, since in those models and structure a CPT derivative with an A-ring 10-OH would not interact with Asn352. It is important to note that topotecan is positively charged, and this is a key factor for its intercalation into DNA independently of top1, and perhaps also for its intercalation mode of inhibiting top1 (*31*).

All other residues circling the top1/DNA active site, which are within H-bonding distance of the docked SN-38, have been shown to either be important for inhibitor binding or be essential for top1 activity (Results and Discussion). Interestingly, while Glu356, Asn430 (not shown), and Lys751 are out of direct H-bonding range of CPT and SN-38 (Figure 2A), future derivatives of CPT could be designed to exploit H-bond interactions with these residues and so enhance inhibitor binding to the top1/DNA active site. The top1-resistant mutants F361S and G363C (*68*, *69*) are removed from direct interactions with CPT in this model, and in the three previous models. These resistance mutations' actions are probably due to their altering the orientation of the loop that contains Arg364 (*9*).

The present experimentally tested model furthers our understanding of top1/inhibitor interactions, and can be further tested since it predicts as yet unused top1 residues with which novel derivatives of CPT could be designed to interact. Together, these results will promote the search for, and development of, novel CPT derivatives with higher therapeutic indices in the fight against cancer.

ACKNOWLEDGMENT

We thank Dr. Ajay for his advice, Glenda Kohlhagen for her technical help, as well as Drs. Monroe Wall, Mansukh C. Wani, and Dennis P. Curran for their thoughtful help.

REFERENCES

1. Champoux, J. (1990) in *DNA topology and its biological effects* (Wang, J. C., and Cozarelli, N. R., Eds.) pp 217−242, Cold Spring Harbor Laboratory, Cold Spring Harbor, NY.
2. Pommier, Y., and Tanizawa, A. (1993) in *Cancer Chemotherapy* (Hickman, J., and Tritton, T., Eds.) pp 214−250, Blackwell Scientific Publications Ltd., Oxford.
3. Chen, A. Y., and Liu, L. F. (1994) *Annu. Rev. Pharmacol. Toxicol. 94*, 194−218.
4. Wall, M. E., Wani, M. C., Cooke, C. E., Palmer, K. H., McPhail, A. T., and Slim, G. A. (1966) *J. Am. Chem. Soc. 88*, 3888−3890.
5. Ozols, R. F. (2000) *Int. J. Gynecol. Cancer 10*, 33−37.
6. Saltz, L. B., Cox, J. V., Blanke, C., Rosen, L. S., Fehrenbacher, L., Moore, M. J., Maroun, J. A., Ackland, S. P., Locker, P. K., Pirotta, N., Elfring, G. L., and Miller, L. L. (2000) *N. Engl. J. Med. 343*, 905−914.
7. Wang, J. C. (1996) *Annu. Rev. Biochem. 65*, 635−692.

8. Champoux, J. J. (1998) *Prog. Nucleic. Acid Res. Mol. Biol. 60*, 111−132.
9. Redinbo, M. R., Stewart, L., Kuhn, P., Champoux, J. J., and Hol, W. G. (1998) *Science 279*, 1504−1513.
10. Hsiang, Y. H., Hertzberg, R., Hecht, S., and Liu, L. F. (1985) *J. Biol. Chem. 260*, 14873−14878.
11. Snapka, R. M., and Permana, P. A. (1993) *Bioessays 15*, 121−127.
12. Tsao, Y. P., Russo, A., Nyamusa, G., Silber, R., and Liu, L. F. (1993) *Cancer Res. 53*, 5908−5914.
13. Strumberg, D., Pilon, A. A., Smith, M., Hickey, R., Malkas, L., and Pommier, Y. (2000) *Mol. Cell. Biol. 20*, 3977−3987.
14. Holm, C., Covey, J. M., Kerrigan, D., and Pommier, Y. (1989) *Cancer Res. 49*, 6365−6368.
15. Hsiang, Y.-H., Lihou, M. G., and Liu, L. F. (1989) *Cancer Res. 49*, 5077−5082.
16. Ryan, A. J., Squires, S., Strutt, H. L., and Johnson, R. T. (1991) *Nucleic Acids Res. 19*, 3295−3300.
17. Pommier, Y., Pourquier, P., Urasaki, Y., Wu, J., and Laco, G. S. (1999) *Drug Resistance Updates 2*, 307−318.
18. Pommier, Y., Laco, G. S., Kohlhagen, G., Sayer, J. M., Kroth, H., and Jerina, D. M. (2000) *Proc. Natl. Acad. Sci. U.S.A. 97*, 10739−10744.
19. Pommier, Y., Kohlhagen, G., Pourquier, P., Sayer, J. M., Kroth, H., and Jerina, D. M. (2000) *Proc. Natl. Acad. Sci. U.S.A. 97*, 2040−2045.
20. Geacintov, N. E., Cosman, M., Hingerty, B. E., Amin, S., Broyde, S., and Patel, D. J. (1997) *Chem. Res. Toxicol. 10*, 111−146.
21. Volk, D. E., Rice, J. S., Luxon, B. A., Yeh, H. J. C., Liang, C., Xie, G., Sayer, J. M., Jerina, D. M., and Gorenstein, D. G. (2000) *Biochemistry 39*, 14040−14053.
22. Fan, Y., Weinstein, J. N., Kohn, K. W., Shi, L. M., and Pommier, Y. (1998) *J. Med. Chem. 41*, 2216−2226.
23. Klimasauskas, S., Kumar, S., Roberts, R. J., and Cheng, X. (1994) *Cell 76*, 357−369.
24. Lau, A. Y., Scharer, O. D., Samson, L., Verdine, G. L., and Ellenberger, T. (1998) *Cell 95*, 249−258.
25. Barrett, T. E., Scharer, O. D., Savva, R., Brown, T., Jiricny, J., Verdine, G. L., and Pearl, L. H. (1999) *EMBO J. 18*, 6599−6609.
26. Kerrigan, J. E., and Pilch, D. S. (2001) *Biochemistry 40*, 9792−9798.
27. Yoshimasa, U., Laco, G. S., Pourquier, P., Takebayashi, Y., Kohlhagen, G., Giofre, C., Chatterjee, D., Pantazis, P., and Pommier, Y. (2001) *Cancer Res.* (in press).
28. Andoh, T., Ishii, K., Suzuki, Y., Ikegami, Y., Kusunoki, Y., Takemoto, Y., and Okada, K. (1987) *Proc. Natl. Acad. Sci. U.S.A. 84*, 5565−5569.
29. Tamura, H., Kohchi, C., Yamada, R., Ikeda, T., Koiwai, O., Patterson, E., Keene, J. D., Okada, K., Kjeldsen, E., Nishikawa, K., and Andoh, T. (1991) *Nucleic Acids Res. 19*, 69−75.
30. Fujimori, A., Harker, W. G., Kohlhagen, G., Hoki, Y., and Pommier, Y. (1995) *Cancer Res. 55*, 1339−1346.
31. Stewart, L., Staker, B., Hjerrild, K., Burgin, A., and Kim, H. (2001) *American Association for Cancer Research 92nd Annual Meeting*, Abstract LB-43.
32. Yang, D., Strode, J. T., Spielmann, H. P., Wang, A., and Burke, T. G. (1998) *J. Am. Chem. Soc. 120*, 2979−2980.
33. Yao, S., Murali, D., Seetharamulu, P., Haridas, K., Petluru, P. N., Reddy, D. G., and Hausheer, F. H. (1998) *Cancer Res 58*, 3782−3786.
34. Pommier, Y. (1998) *Biochimie 80*, 255−270.
35. Crow, R. T., and Crothers, D. M. (1992) *J. Med. Chem. 35*, 4160−4164.
36. Pourquier, P., Takebayashi, Y., Urasaki, Y., Gioffre, C., Kohlhagen, G., and Pommier, Y. (2000) *Proc. Natl. Acad. Sci. U.S.A. 97*, 1885−1890.
37. Zhelkovsky, A. M., Moore, C. L., Rattner, J. B., Hendzel, M. J., Furbee, C. S., Muller, M. T., and Bazett-Jones, D. P. (1994) *Protein Expression Purif. 5*, 364−370.
38. Pourquier, P., Pilon, A. A., Kohlhagen, G., Mazumder, A., Sharma, A., and Pommier, Y. (1997) *J. Biol. Chem. 272*, 26441−26447.
39. Bonven, B. J., Gocke, E., and Westergaard, O. (1985) *Cell 41*, 541−551.
40. Eritja, R., Walker, P. A., Randall, S. K., Goodman, M. F., and Kaplan, B. E. (1987) *Nucleosides Nucleotides 6*, 803−814.
41. Beaucage, S. L. (1993) *Methods Mol. Biol. (Totowa, N.J.) 20*, 33−61.
42. Warner, D. L., and Burke, T. G. (1997) *J. Chromatogr., B: Biomed. Sci. Appl. 691*, 161−171.
43. Momany, F. A., McGuire, R. F., Burgess, A. W., and Scheraga, H. A. (1975) *J. Phys. Chem. 79*, 2361−2381.
44. Scheraga, H. A., Department of Chemistry, Indiana University, Bloomington, IN.
45. Stewart, J. J. P., Quantum Chemistry Program Exchange, Indiana University, Bloomington, IN.
46. Luke, B. T. (1996) in *Principles in QSAR and Drug Design* (Devillers, J., Ed.) Academic Press Ltd., London.
47. Powell, M. J. D. (1964) *Comput. J. 7*, 155−162.
48. Cornell, W. D., Cieplak, P., Bayly, C. I., Gould, I. R., Merz, K. M. J., Ferguson, D. M., Spellmeyer, D. C., Fox, T., Caldwell, J. W., and Kollman, P. A. (1995) *J. Am. Chem. Soc. 117*, 5179−5197.
49. Wang, J., Cieplak, P., and Kollman, P. A. (2000) *J. Comput. Chem. 21*, 1049−1074.
50. Case, D. A., Pearlman, D. A., Caldwell, J. W., Cheatham, T. E., III, Ross, W. S., Simmerling, C. L., Darden, T. A., Merz, K. M., Stanton, R. V., Cheng, A. L., Vincent, J. J., Crowley, M., Tsui, V., Radmer, R. J., Duan, Y., Pitera, J., Massova, I., Seibel, G. L., Singh, U. C., Weiner, P. K., and Kollman, P. A. (1999) University of California, San Francisco.
51. UniChem., Oxford Molecular, Medawar Centre, Oxford Science Park, Oxford, OX4 4GA, England.
52. Jaxel, C., Kohn, K. W., Wani, M. C., Wall, M. E., and Pommier, Y. (1989) *Cancer Res. 49*, 1465−1469.
53. Hsiang, Y.-H., Liu, L. F., Wall, M. E., Wani, M. C., Nicholas, A. W., Manikumar, G., Kirschenbaum, S., Silber, R., and Potmesil, M. (1989) *Cancer Res. 49*, 4385−4389.
54. Giovanella, B. C., Stehlin, J. S., Wall, M. E., Wani, M. C., Nicholas, A. W., Liu, L. F., Silber, R., and Potmesil, M. (1989) *Science 246*, 1046−1048.
55. Pommier, Y., Tanizawa, A., and Kohn, K. W. (1994) *Adv. Pharmacol. 29B*, 73−92.
56. Pourquier, P., Ueng, L. M., Kohlhagen, G., Mazumder, A., Gupta, M., Kohn, K. W., and Pommier, Y. (1997) *J. Biol. Chem. 272*, 7792−7796.
57. Mi, Z., and Burke, T. G. (1994) *Biochemistry 33*, 10325−10336.
58. Fassberg, J., and Stella, V. J. (1992) *J. Pharm. Sci. 81*, 676−684.
59. Leteurtre, F., Fesen, M., Kohlhagen, G., Kohn, K. W., and Pommier, Y. (1993) *Biochemistry 32*, 8955−8962.
60. Hertzberg, R. P., Caranfa, M. J., and Hecht, S. M. (1989) *Biochemistry 28*, 4629−4638.
61. Tanizawa, A., Kohn, K. W., Kohlhagen, G., Leteurtre, F., and Pommier, Y. (1995) *Biochemistry 34*, 7200−7206.
62. Jensen, A. D., and Svejstrup, J. Q. (1996) *Eur. J. Biochem. 236*, 389−394.
63. Wang, X., Zhou, X., and Hecht, S. M. (1999) *Biochemistry 38*, 4374−4381.
64. Gromova, I. I., Kjeldsen, E., Svejstrup, J. Q., Alsner, J., Christiansen, K., and Westergaard, O. (1993) *Nucleic Acids Res. 21*, 593−600.
65. Ejima, A., Terasawa, H., Sugimori, M., Ohsuki, S., Matsumoto, K., Kawato, Y., Yasuoka, M., and Tagawa, H. (1992) *Chem. Pharm. Bull. (Tokyo) 40*, 683−688.
66. Pommier, Y., Kohlhagen, G., Kohn, K. W., Leteurtre, F., Wani, M. C., and Wall, M. E. (1995) *Proc. Natl. Acad. Sci. U.S.A. 92*, 8861−8865.
67. Stewart, L., Redinbo, M. R., Qiu, X., Hol, W. G., and Champoux, J. J. (1998) *Science 279*, 1534−1541.
68. Rubin, E., Pantazis, P., Toppmeyer, D., Giovanella, B., and Kufe, D. (1994) *J. Biol. Chem. 269*, 2433−2439.
69. Benedetti, P., Fioranti, P., Capuani, L., and Wang, J. C. (1993) *Cancer Res. 53*, 4343−4348.

BI011774A